

# Combinatorial peel tests for the characterization of adhesion behavior of polymeric films<sup>☆</sup>

R. Song<sup>a,1</sup>, M.Y.M. Chiang<sup>a,\*</sup>, A.J. Crosby<sup>a,2</sup>, A. Karim<sup>a</sup>, E.J. Amis<sup>a</sup>, N. Eidelman<sup>b</sup>

<sup>a</sup>*Polymer Division, National Institute of Standards and Technology, Gaithersburg, MD 20899, USA*

<sup>b</sup>*Paffenbarger Research Center, American Dental Association Foundation, Gaithersburg, MD 20899, USA*

Received 16 November 2003; received in revised form 24 September 2004; accepted 5 October 2004

Available online 13 January 2005

## Abstract

The adhesion behavior of an optically smooth poly(methyl methacrylate) (PMMA) thin film (100 nm in thickness) on different evaporated metal substrates has been investigated using a combinatorial method approach. In this investigation through high-throughput peel tests, the relationship between annealing time, annealing temperature, surface energy, and ultraviolet degradation to the film adhesion has been examined. In addition, atomic force microscopy, optical microscopy and Fourier transform infrared microspectroscopy techniques have been adopted to elucidate the observations on the adhesion behavior from the peel tests. The results of this study demonstrate that the proposed combinatorial approach to characterize the dependence of adhesion on adhesion-controlling parameters has the potential to assess various factors affecting the adhesion.

Published by Elsevier Ltd.

*Keywords:* Combinatorial method; Adhesion; PMMA

## 1. Introduction

Polymer adhesion is studied extensively because of important applications in industrial processes, such as composite manufacturing and durability, coatings, biomedical devices and implants, and packaging for microelectronics components. Current (traditional) approaches to the characterization of adhesion have focused on attempts to isolate a single adhesion-controlling parameter and monitor the changes in adhesion with changes in that single parameter. However, this methodology is time consuming, discrete, and does not allow interplay between variables to be investigated. In this work, we present results of adhesion

characterization for polymer/substrate systems using combinatorial methodologies. The ultimate goals of this research are to develop techniques for processing and analyzing multi-variables of the interface and to map the dependence of adhesion on these adhesion-controlling parameters rapidly, practically, and efficiently.

Recently, combinatorial methods have presented a paradigm for efficient polymer synthesis, characterization and curing. The revival of combinatorial methods within materials science has recently moved from inorganic [1–6] to organic and polymeric materials [7–21]. Several novel methods have emerged for the preparation of polymer film libraries with continuous gradients in temperature, composition, thickness and surface energy, which make our current research available. From these libraries, several high-throughput screening methods have been demonstrated for cell–polymer interaction [14], polymer-blend phase behavior [15], block-copolymer segregation [16], and adhesion reliability [17–19,21]. Stimulated by the initial success in some fields of polymer characterization, we extend the combinatorial technique to polymer adhesion.

In this study through peel tests, in which the force

<sup>☆</sup> Official contribution of the National Institute of Standards and Technology; not subject to copyright in the United States.

\* Corresponding author. Tel.: +1 301 975 5186.

*E-mail address:* [martin.chiang@nist.gov](mailto:martin.chiang@nist.gov) (M.Y.M. Chiang).

<sup>1</sup> Present address: State Key Laboratory of Polymer Physics and Chemistry, Center of Molecular Science, Institute of Chemistry, Chinese Academy of Sciences, Beijing 100080, China.

<sup>2</sup> Present address: Polymer Science and Engineering Department, University of Massachusetts, Amherst, MA 01003, USA.

required to peel a test film from a test substrate is recorded and gives a measure of adhesion (the peel energy for debonding the film from the substrate), we present a high-throughput (combinatorial) approach to study the effects of polymer annealing temperature and time on adhesion development for different substrates. Also, the relationship between the annealing time, annealing temperature, surface energy, and ultraviolet (UV) degradation to the film adhesion has been examined using the combinatorial approach. Poly (methyl methacrylate) (PMMA) has been selected as the subject polymer, since it can be easily prepared into a uniform thin film and is relatively stable upon heating. Silicon, aluminum, chromium, copper and gold have been used as the substrate.

## 2. Materials and experiments<sup>3</sup>

### 2.1. Film samples and substrate preparation

The PMMA sample (from Polysciences, Inc, Warrington, PA, USA) used in this study has a molar mass and polydispersity of 100,000 g/mol and 2.26, respectively. Preliminary test indicated that it has a glass transition temperature ( $T_g$ ) of ca. 105 °C (probed by differential scanning calorimeter (DSC) with a heating rate of 20 °C/min). The PMMA solution in chloroform (5% by mass fraction) was spin-coated on a silicon substrate at 4 rad/s for 30 s to form a PMMA film (ca. 100 nm in thickness) on a silicon substrate. The resulting film was removed from the substrate by floating in water and transferred to a selected substrate. By using this process, the bonding strength of such film on a substrate can be evaluated by a peel test at the early stages of annealing since the interfacial strength is relatively low.

In this study, PMMA films were placed on silicon wafers (Polishing Corporation of American, CA) and on silicon wafers coated with thin metal layers of Au, Al, Cr, and Co, to mimic different substrates such that their effects on the adhesion can be investigated. These metal layers were deposited on the silicon wafer using a thermal evaporator (Granville-Phillips Company, Boulder, CO) at a pressure of less than 0.2 Pa. It should be noted that in the thermal evaporation technique, the average energy of vapor atoms reaching the substrate is generally low (order of  $kT$ , i.e. tenths of eV). This can seriously affect the morphology of the metal layer and often results in a porous and weak adherent layer. The PMMA film thickness was measured after solidification using a UV reflectance interferometer F20 (Filmetrics, San Diego, CA) with a 0.5 mm diameter

spot size, and corroborated by a Dektak 8 stylus profiler (Veeco Co, Santa Barbara, CA). Over the range of 10–100 nm in length, the thickness measurement using the reflectance interferometer agrees with the thickness measurement obtained from the profiler within 4% discrepancy (the standard uncertainty is  $\pm 0.05 \mu\text{m}$ ).

In addition, we deposited PMMA films on silicon substrates having an alkylsilane self-assembled monolayer (SAM), and the surfaces of these SAM-coated substrates were UV-modified to introduce different surface energy levels. Procedures that are critical to the film/substrate system preparation include cleaning the substrate, the formation of a SAM and a desired contact angle gradient (surface energy gradient).

### 2.2. Formation of a SAM layer and a contact angle gradient

A polished silicon wafer (100) with a 1–2 nm thick native oxide layer was cut into a rectangle (30 mm  $\times$  50 mm) and thoroughly cleaned prior to introducing a self-assembly monolayer (SAM) with a surface energy gradient on its surface. The silicon wafer was air-cleaned with nitrogen to remove dust and sequentially ultrasonic-cleaned in acetone, 2-propanol, and deionized, ultra filtered water (with a resistance exceeding  $18 \text{ M}\Omega \text{ cm}^{-1}$ ). The wafer was dried with nitrogen between these ultrasonic-cleaning steps. After the cleaning process, the wafer was placed into a UVO (UV Ozone) cleaner (Model 342 UV Cleaner, Jelight Company, Inc., Irvine, CA) for 15 min to generate a more uniform silicon oxide layer, rinsed with water, and dried with nitrogen. Afterwards, the wafer was etched with buffered HF for approximately 30 s to remove the oxide layer and leave an exposed hydrophobic Si–H layer on the surface of the silicon wafer. The wafer was rinsed with water, dried with nitrogen, and returned to the UVO cleaner for 3 min. Finally the wafer was washed and dried again before the SAM formation.

It is possible to obtain a finely tuned or chemically-patterned surface using photochemical oxidation for surface modifications of a SAM-coated substrate [13]. In this study, we used a reactive alkylsilane and a controlled UV exposure density to obtain a SAM with a surface energy gradient on the substrate. As investigated previously, the use of reactive alkylsilane to modify the surface properties of inorganic materials is a widely accepted process [14]. In the preparation of the SAM, both a solution method and a vapor method were adopted in this study. In the case of the solution method, a cleaned substrate was submerged for approximately 30 min in a solution mixture (2.5% by mass fraction) made from 1 g of *n*-octyldimethylchlorosilane (*n*-ODCS, used as received from Gelest Inc., Morrisville, PA) and 39 g of toluene. Afterwards, the wafer was rinsed with toluene and dried with nitrogen before annealing in an oven at 120 °C for more than 1 h. After the annealing step, the coated substrate was washed with toluene and dried again with nitrogen. In the vapor deposition method, the wafer

<sup>3</sup> Certain equipments and instruments or materials are identified in the paper in order to adequately specify the experimental details. Such identification does not imply recommendation by the National Institute of Standards and Technology, nor does it imply the materials are necessarily the best available for the purpose.

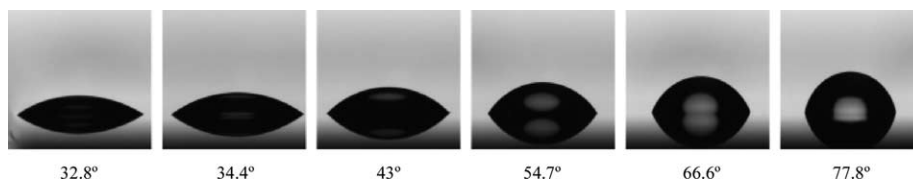


Fig. 1. Optical images of a contact angle gradient for water droplets on a silicon substrate having a SAM layer exposed to a UV gradient; the distance between two droplets is 8 mm.

was kept overnight in a vacuum desiccator filled with silane vapor at room temperature. It was then thoroughly rinsed with toluene and dried with nitrogen as usual. Generally, a more uniform layer can be achieved using the vapor method than the solution method. A detailed description of the vapor method can be found elsewhere [14].

After the SAM formation, the wafer was placed into a UVO device developed in our laboratory for generating a contact angle gradient (the irradiation intensity is  $400 \mu\text{W}/\text{cm}^2$  at 360 nm), and more detailed procedures can be found in the literature [21]. Theoretically, the larger the UV dose, the lower the water contact angle (higher the surface energy, lower the hydrophobicity) will be. In this study, the resulting contact angles normally ranged continuously from 30 to 80° (the standard uncertainty is within  $\pm 1^\circ$ ), as given in Fig. 1, for a 3 min UVO treatment. The contact angle measurement was performed with a G2 video contact angle system (Kruss Corp., Hamburg, Germany) at room temperature using high purity water as a probing solvent.

### 2.3. Temperature gradient stage and peel tests

An aluminum plate,  $(102 \times 62 \times 4) \text{ mm}^3$ , having a temperature gradient was used as a temperature stage for studying the annealing temperature effect on the development of adhesion between a film and a substrate. One edge of the plate has a higher temperature from a metal heating bar controlled by a thermal controller, and the opposite edge has a lower temperature from a refrigerating bath circulator (RTE-220, Neslab, Newington, NH) filled with constant temperature fluid. This setup can offer a controllable temperature range from 30 to 240 °C with fluctuations less than  $\pm 2^\circ\text{C}$ . The film/substrate sample is placed on a location in the temperature stage based on a desired temperature gradient.

The adhesion of a film/substrate interface was evaluated in terms of the peel energy ( $G_{\text{IC}}$ ) using a peel test [23] on the TX.XT2I texture analyzer (Stable Micro System, Surrey, UK). The test was carried out at ambient temperature by peeling a commercial tape (3M) adhered to the PMMA of the film/substrate sample at 180° peel angle and a 1.0 mm/s peel rate (Fig. 2). The backing tape was grabbed for peeling, since the test film was very thin (ca. 100 nm in thickness) such that a direct peeling of the film from the substrate is impossible. The adhesion between the tape and the film is

assumed to be stronger than that between the film and the substrate. Results from separate experiments (not reported here) indicate that the assumption is valid. To obtain an intimate contact between the tape and the film, the air bubbles between the tape and the film/substrate sample were squeezed out with a blunt knife-edge and cotton swabs. If the extension of the peel strip (PMMA film and the tape) is negligible, the  $G_{\text{IC}}$  can be determined through the following equation:

$$G_{\text{IC}} = P(1 - \cos \theta)/b = 2P/b \quad (\text{for } \theta = 180^\circ) \quad (1)$$

where  $P$  is the peel force, and  $b$  is the width of the test sample. In our study, the  $G_{\text{IC}}$  was obtained from the average of at least 3 peel tests per film/substrate system.

### 2.4. UV degradation, AFM, and FTIR

For the UV degradation experiment, a UVO (UV Ozone) cleaner (Model 342 UV Cleaner, described in the above section) was used. A PMMA thin film deposited on the Si substrate ( $2.5 \text{ cm} \times 7.5 \text{ cm}$ ) was placed in the UV cleaner for treatment. The PMMA/Si sample was ink-marked in different locations to form 7 regions. These regions were under the same intensity of UV irradiation for varying exposure times (2, 4, 8, 16, 32, 64 min; one region was reserved for no irradiation). Right after each exposure time, an exposed region was covered with a metal plate. By repeating such a procedure, each region had a different UV exposure time. Consequently, a UV degradation gradient due to different exposure times would be produced on the sample. The surface of the degraded sample was subsequently characterized using AFM, optical microscopy, and FTIR microspectroscopy techniques.

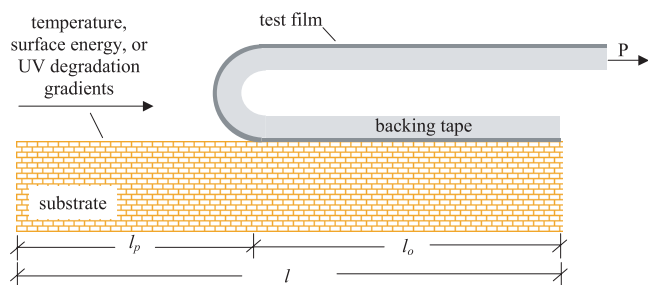


Fig. 2. Schematic of peel test for peeling a commercial tape (as a backing tape) adhered to a test film at 180° peel angle.  $l$  is the original sample (bonded) length.  $l_p$  is the peeled length.  $l_o$  is the bonded length after peeling.

In order to correlate the peel force with the surface roughness of the PMMA coated substrate, the surfaces of the coated substrates were imaged using atomic force microscopy (AFM) and optical microscopy. All the AFM images were recorded with a Dimension 3100 microscope (Digital Instruments Inc.) operated in tapping mode with a spring constant of  $\approx 30$  N/m at room temperature. To check the reproducibility of the observed roughness, at least 4 samples of each composition were probed.

Optical microscopy was also utilized to characterize the sample surface. A Kodak Megaplug camera ( $1024 \times 1024$ ), 8 bit pixels was connected to a Nikon Optiphot 2 microscope operating in reflection mode. The microscope's standard sample stage was replaced with a motorized two-dimensional translation stage possessing a 5 cm range of motion and a  $0.5 \mu\text{m}$  resolution. A computer synchronously controlled the translation stage and acquired digital images from the CCD while scanning across the samples.

To elucidate chemical changes in polymer structure due to the UV irradiation exposure, Fourier transform infrared microspectroscopy was used. Applying FTIR microspectroscopy in reflectance mode to thin films coated reflective substrates, results in reflection-transmission spectra (FTIR-RTM). These spectra are equivalent to traditional absorption spectra after converting them to absorbance without any mathematical correction [22]. FTIR-RTM was applied in this study to PMMA films deposited on Al coated Si substrate. Nicolet Magna-IR 550 FTIR spectrophotometer interfaced with a Nic-Plan IR microscope was used. The microscope is equipped with a video camera, a liquid nitrogen cooled-mercury cadmium telluride (MCT/A) detector (Nicolet Instrumentations Inc. Madison, WI, USA) and a computer-controlled mapping stage (Spectra-Tech, Inc., Shelton, CT, USA), programmable in the  $x$  and  $y$  directions. The spectral point-by-point mapping of the PMMA film was performed in a grid pattern with the computer-controlled microscope stage and Omnic Atlas software. The film was mapped at every  $300 \mu\text{m}$  across the gradient direction ( $x$ -axis), and every  $2000 \mu\text{m}$  across the presumed constant  $y$ -axis direction. The spectra were collected from  $4000$  to  $650 \text{ cm}^{-1}$  at a spectral resolution of  $8 \text{ cm}^{-1}$  with 16 scans per spectrum and beam spot size of  $300 \times 300 \mu\text{m}^2$ , and were proportioned against a gold coated disk. The map was processed as ratios between the area of the CO peak (spectral region:  $1660$ – $1820 \text{ cm}^{-1}$ ) and the COCH<sub>3</sub> group (spectral region:  $1050$ – $1330 \text{ cm}^{-1}$ ) and displayed as a color contour map. The map was imported into the recently revised ISys software (Spectra Dimensions, Olney, MD), and the ratios between the integrated areas under the CO and COCH<sub>3</sub> groups were acquired for each spectrum of the map. Averages and standard deviations were calculated for each step along the gradient ( $300 \mu\text{m}$ ).

### 3. Results and discussion

#### 3.1. Effect of annealing time and temperature on adhesion development

In order to examine the role of heat diffusion in the development of polymer adhesion to a substrate, samples of the PMMA/Al system annealed with a temperature gradient were subjected to peel tests to characterize the adhesion behavior. Three annealing temperature gradients (ranging from  $83$  to  $170 \text{ }^\circ\text{C}$ ,  $88$  to  $180 \text{ }^\circ\text{C}$ , and  $93$  to  $193 \text{ }^\circ\text{C}$ ) were applied to samples annealed for various time ranging from 10 min to 12 h. The peel test was conducted at a constant load and rate for the samples with the same annealing temperature gradient. After the loading, the PMMA film would be peeled from the substrate to a certain position (Fig. 2), and the remaining bonded length of the film,  $l_0$ , (Fig. 2) was recorded for a specific annealing time. Afterwards, a critical temperature,  $T_c$ , is determined based on the  $l_0$ , the original bonded length, and the temperature gradient that the sample has been subjected to. Fig. 3 shows typical variations of the  $l_0$  and  $T_c$  as a function of annealing time for an annealing temperature gradient from  $93$  to  $193 \text{ }^\circ\text{C}$ . Within the temperature gradients studied, all the results on the development of PMMA adhesion to Al exhibit similar trends and can be achieved at relatively low temperatures. Also, the results in the figure qualitatively express the significance of time–temperature dependence on the adhesion development.

Fig. 4 gives the variation of  $T_c$  with annealing time for PMMA films with different metal substrates subjected to a temperature gradient from  $85$  to  $180 \text{ }^\circ\text{C}$ . For these film/metal systems, the loads and loading rates adopted in the peel tests remained constant. The results in the figure suggest that the aforementioned time–temperature relationship is a common feature for any metal substrates (i.e. Cr, Cu and Au) employed with PMMA. Also, the adhesion behavior of PMMA to the substrate displays a profound

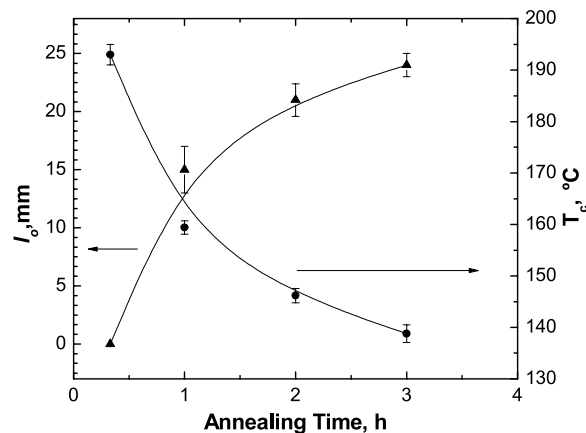


Fig. 3. Typical variations of the unbroken length,  $l_0$  (▲, mm) and critical temperature,  $T_c$  (●,  $^\circ\text{C}$ ) as a function of annealing time ( $h$ ) for an annealing temperature gradient of  $93$ – $193 \text{ }^\circ\text{C}$ .

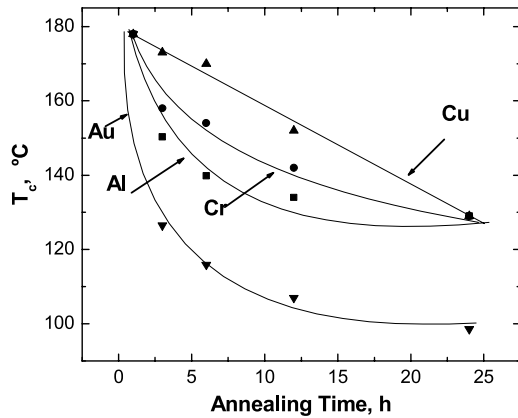


Fig. 4. Variation of critical temperature,  $T_c$ , as a function of annealing time for different metal substrates. The annealing temperature gradient is from 85 to 180 °C.

dependence on the metal layer. The region above each curve in the figure can be regarded as a bonded area while the region below the curve revealed as a debonded area. Each curve represents a distribution of failure (failure map) as a function of annealing temperature and time for the PMMA film peeled at 180° from the corresponding substrate. Although more research is needed, the results in the figure suggest that the PMMA forms the strongest adhesion to the Cu and the weakest adhesion to the Au coated substrate. This dependence of the adhesion of PMMA on the metallic nature of the substrate could be partially attributed to the differences in wettability and roughness of the substrates, which are beyond the scope of this study.

The adhesion depends not only on the intrinsic properties of the respective substrate, but also on many other variables involved in the film preparation, such as the solvent, polymer concentration, molecular mass and its distribution, etc. In this study, the adhesion behavior of silicon and PMMA films, which were prepared with two different solvents (chloroform and toluene), will be discussed. These two solvents are generally viewed as a good solvent and a poor solvent, respectively, for PMMA. Fig. 5 presents the  $T_c$  as a function of annealing time for PMMA films produced with these two solvents. As suggested from higher  $T_c$  values for a specific annealing time, one can see that PMMA samples prepared with toluene tend to bond better than those prepared with chloroform. This difference in the adhesion can be attributed partially to the volatility of the solvents employed, which can be critical for obtaining smooth ultra-thin films [24]. This argument can be demonstrated using RMS roughness measured for the PMMA films with toluene and chloroform (i.e.  $2.4 \pm 0.5$  nm and  $7.5 \pm 1.2$  nm, respectively, over  $10 \mu\text{m} \times 10 \mu\text{m}$  measurement). The difference in roughness could be due to more residual solvent being left during the spin coating process for the PMMA film with toluene than with chloroform. The roughness can be altered in the subsequent annealing process but the samples prepared from toluene tend to have lower values than

those from chloroform. Another argument on the influence of solvents on the  $T_c$  could be attributed to the mobility of PMMA molecular chain. Although the silicon was used as a substrate in this case, the findings presented in the figure should be applicable to any other substrates.

### 3.2. Relationship between surface energy and annealing time and temperature in adhesion development

As the surface wettability (surface energy) of the substrate usually affects the solid/liquid adhesion, it is worthwhile to use a combinatorial approach to study the effect of the contact angle, annealing time and annealing temperature on the peel strength. Fig. 6(a) displays the variation of the critical contact angle ( $\theta_c$ , which will be defined later) with the annealing time for different constant annealing temperatures. In this case, a sample of a PMMA film, deposited on a silicon substrate having a contact angle gradient, was annealed at a specific temperature for a specific time period. Then, a constant peel force was applied to the sample starting from the sample end having a largest contact angle. Consequently, the PMMA film would be partially peeled from the substrate, and a contact angle corresponding to the bonded length ( $l_o$ ) is obtained. This contact angle is defined as  $\theta_c$ . One can note from the results in Fig. 6(a) that the dependence of  $\theta_c$  on the annealing time becomes less obvious when the annealing time increases. Also, with the increase in the annealing time, the  $l_o$  becomes larger (i.e. a larger  $l_o$  corresponds to a higher contact angle—more hydrophobic part was left on the substrate). In other words, the PMMA tends to adhere to a surface area with lower contact angles (more hydrophilic area) [25]. This argument is reasonable since the polar species of PMMA prefers to interact with the polar groups of the surface. Therefore, the surface chemistry of the substrate plays a critical role in the adhesion of PMMA to a substrate.

If the relationship between the annealing time–temperature and the adhesion observed in Fig. 6(a) can be treated with the time–temperature superposition principle for the

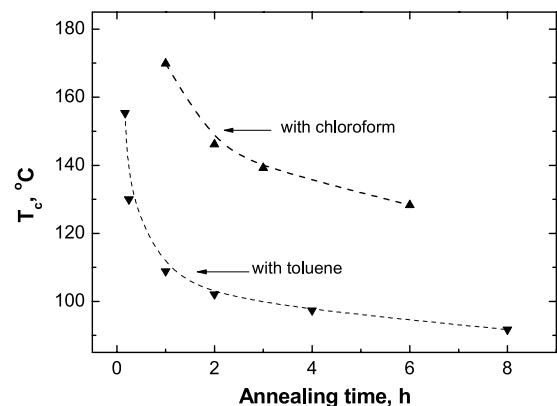


Fig. 5. The dependence of  $T_c$  on the annealing time for PMMA thin films spin-coated with 5% mass fraction of toluene solution and with 5% mass fraction of chloroform solution.

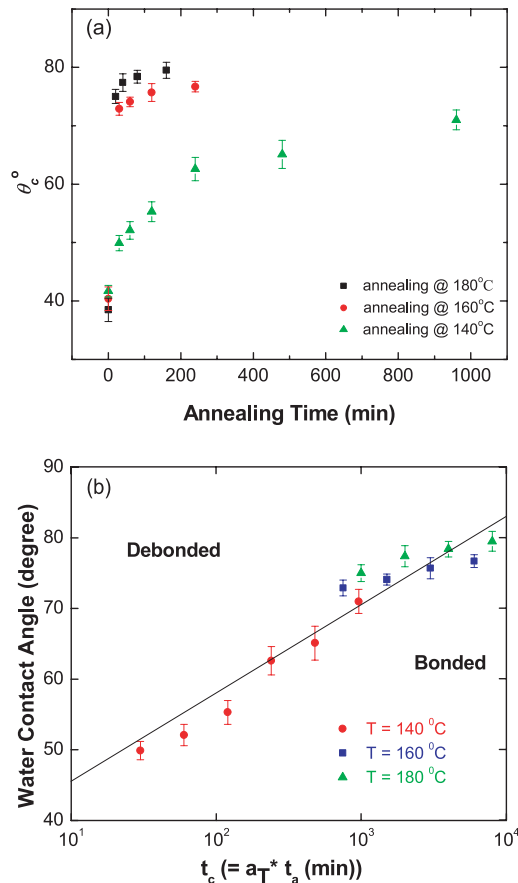


Fig. 6. The critical contact angle gradient,  $\theta_c$ , as a function of annealing time for various annealing temperatures (a), the master curve of peel force as function of annealing time and temperature for PMMA films peeled at 180° from silicon substrates (b).

modulus of a viscoelastic material, one may apply this equivalence principle to the annealing time–temperature, such that a correspondent time ( $t_c$ ) for a certain annealing time ( $t_a$ ) is:

$$t_c = a_T t_a \quad (2)$$

where  $a_T$  is the shift factor, and  $a_T$  can be related to temperature ( $T$ ) through the WLF equation [26]:

$$\log a_T = \frac{-C_1(T - T_g)}{C_2 + T - T_g} \quad (3)$$

where  $C_1$  and  $C_2$  are constants and vary rather slightly from polymer to polymer. If taking  $C_1=17.4$  and  $C_2=51.6$  (universal constants) and applying the data in Fig. 6(a) to Eqs. (2) and (3), one can construct a master curve that illustrates the dependence of the critical contact angle (for the film peeled at 180° from the substrate) on the arbitrary choice of annealing time and temperature (Fig. 6(b)). Assuming that the WLF equation is applicable [27], the results in the figure also provide a failure distribution (failure map) as a function of contact angle and annealing temperature and time. This failure map provides designing engineers and manufacturers a tool to determine materials

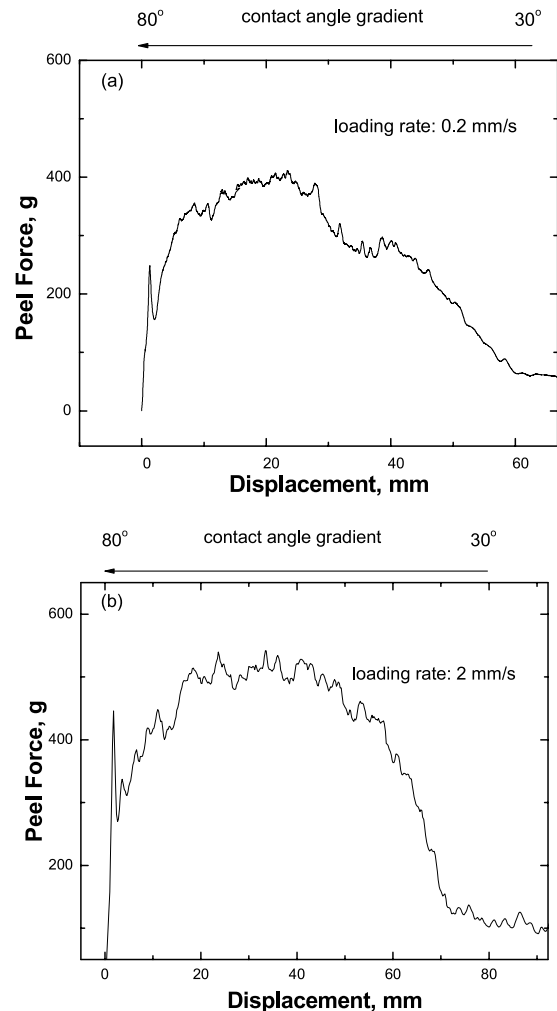


Fig. 7. The force–displacement curve from peel tests of PMMA/silicon samples with different peel rates: 0.2 mm/s (a), 2 mm/s (b).

(or the critical surface energy) needed for practical considerations of the adhesive bond of interest.

Fig. 7(a) presents the peel force ( $P$ )–displacement curve for a peel test of a PMMA/silicon sample, where the silicon substrate has a contact angle gradient ranging from about 30 to 80°. The peel force reaches its maximum in value at a contact angle near 50° and is not directly proportional to the contact angle. This observation on the relationship between peel force and the contact angle can be repeated for different rates (e.g. Fig. 7(b)).

In separate peel tests, commercial tapes (identical to the backing tape used in the previous tests) were directly peeled from different materials with a variety of surface energies at a peel angle of 180°. A plot of the peel force relative to the surface energy of the samples is shown in Fig. 8. These different materials include silicon, glass, aluminum, PMMA, and PTFE (labeled in the figure). The surface energies of those materials listed in the figure were calculated from the measurements of contact angles of a polar fluid (pure H<sub>2</sub>O) and a non-polar fluid (diiodomethane,

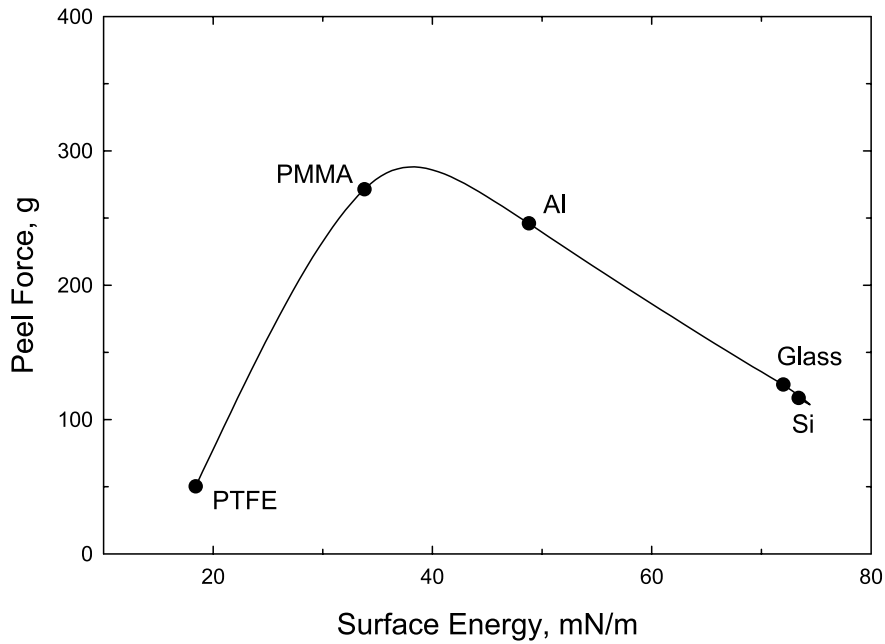


Fig. 8. The Peel force versus surface energy calculated from the Fowkes equation for PTFE, PMMA, Al, glass and Si.

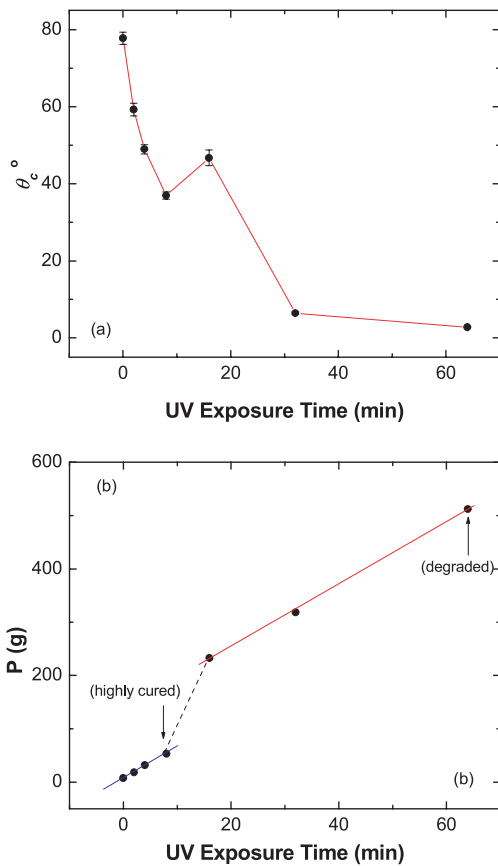


Fig. 9. Variations of water contact angle (a) and peel force (b) as a function of UV exposure time.

CH<sub>2</sub>I<sub>2</sub>) on the corresponding materials, based on the Fowkes equation [28]. Similarly to the results shown in Fig. 7, the results in Fig. 8 also indicate that the peel force is not directly proportional to the contact angle. This is because that the adhesion is not simply controlled by a single parameter, and in this case different degrees of oxidation on various substrate surfaces can also play an important role. Nevertheless, the qualitative similarity between the results in Figs. 7 and 8 validates our findings in using the combinatorial approach. In addition, the peel force for a film peeled from a substrate could be estimated from the contact angle (or surface energy) of the substrate. Conversely, as is usually encountered in field applications, an approximate peel force can be deduced from the probed contact angle.

### 3.3. Interplay of surface energy and UV irradiation on adhesion development

UV irradiation has been widely used in the microelectronic industry to perform circuit photolithography and photoresist curing. It is worthwhile to demonstrate how the combinatorial approach could be applied to explore the influence of the UV exposure on the adhesion between polymers and substrates. In this case, samples made from a PMMA film on silicon substrates with contact angle gradients were exposed to UV irradiation for different periods of time. Upon UV exposure, the PMMA layer undergoes a series of chemical changes, including the initial cross-linking and subsequent degradation induced by the excessive UV dose [29]. Fig. 9 displays the critical contact angle measurement of the sample and the corresponding

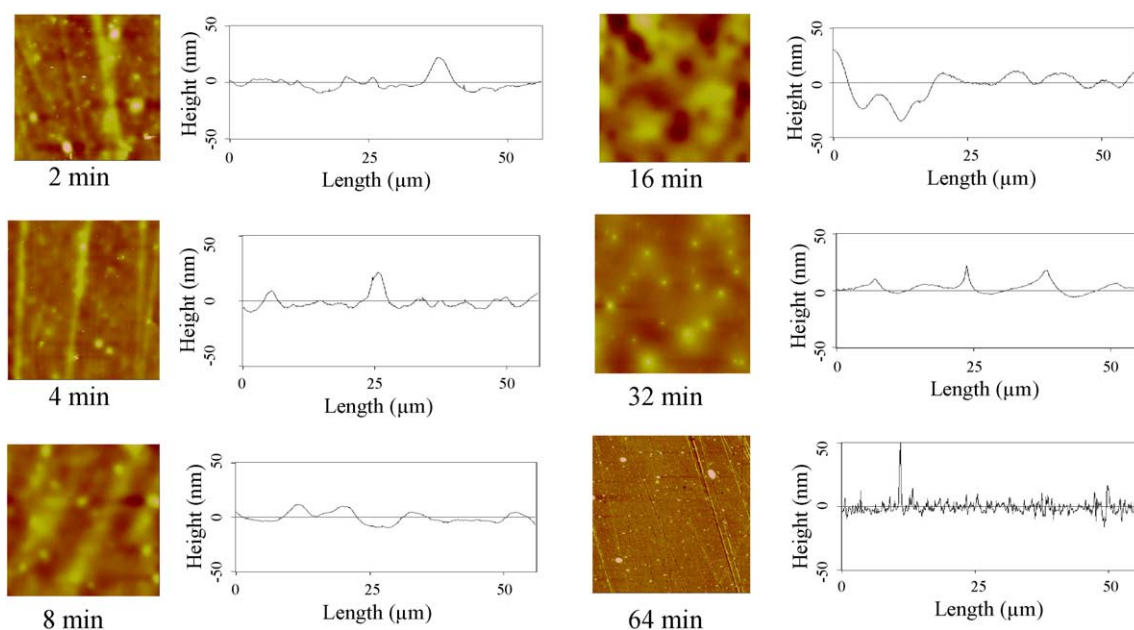


Fig. 10. AFM topography and surface line profile of PMMA film on Al substrate after UV irradiation for various exposure times.

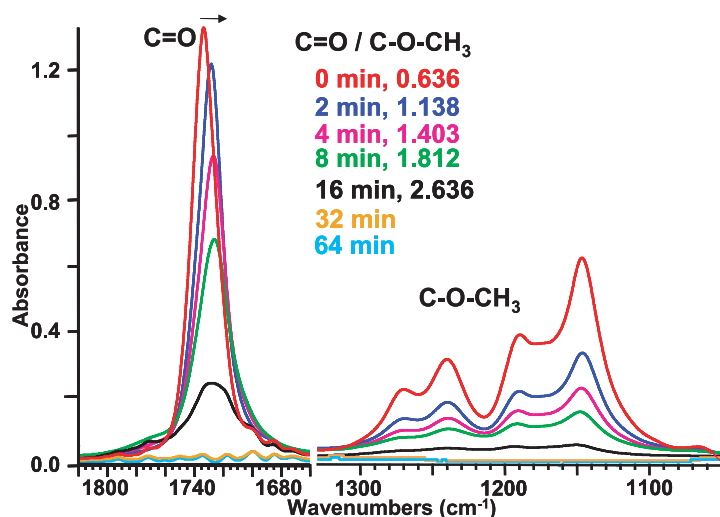
peel force in the test after the UV irradiation as a function of UV exposure time. As indicated in Fig. 9(a), the critical contact angle decreases from ca.  $80^\circ$  to nearly  $0^\circ$  after UV exposure for 64 min (PMMA or the silicon substrate becomes more hydrophilic). Initially, the peel force increases from 4 g (without UV exposure) to 50 g with the decrease of the contact angle (Fig. 9(b)). This force is equivalent to the magnitude of the peel force corresponding to a PMMA/silicon sample cured at  $200^\circ\text{C}$  for 1 h. Upon further UV illumination, the peel force sharply increases since the PMMA has degraded, and the backing tape used in the peel test has a direct contact with the substrate to form a strong bond. Therefore, these forces represent the peel force of the tape from the exposed substrate (not the PMMA film from the substrate). Meanwhile, the morphology of the PMMA film with different UV exposure times can be visualized from AFM topography (Fig. 10), particularly the surface line profile. The results in Fig. 10 suggest that the PMMA would be near fully degraded when radiated for time longer than 16 min, this was manifested as the maximum in roughness data from the topography (10.5 nm of 10  $\mu\text{m}$  scan box). After 64 min of the UV irradiation, the PMMA has completely decomposed (as evidenced by the FTIR data shown in Fig. 11(a)). Also the results in Fig. 10 demonstrate the consistency among the contact angle measurement, the peel force and the morphology of the sample.

FTIR-RTM maps can also provide useful information on the variation of chemical compositions of polymer thin films. FTIR-RTM maps and spectra can be processed as the ratio of different absorbance bands. Representative FTIR spectra that were extracted from the respective time zones in the FTIR-RTM map (Fig. 11(b)) of a PMMA film subjected to different UV exposure times, and the corresponding CO/

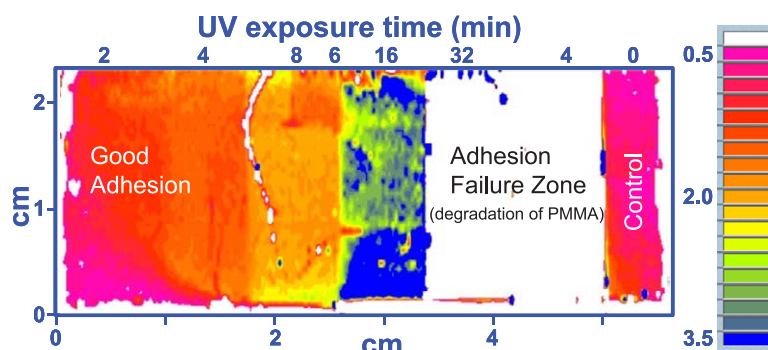
COCH<sub>3</sub> ratios are displayed in Fig. 11(a). The corresponding IR absorption peaks of the carbonyl CO and ether COCH<sub>3</sub> groups of PMMA are depicted separately in the Fig. 11(a). The area ratio of the CO and COCH<sub>3</sub> ( $V_{\text{CO/COCH}_3}$ ) bands, listed in the figure, was used to monitor the variation in the chemical composition during the whole process of UV exposure spanning 0 min to 64 min. The increase in  $V_{\text{CO/COCH}_3}$  from 0.636 to 2.636 during the initial 16 min implies that other carbonyl oxidation products were formed during UV irradiation. Upon further exposure, no detection of the CO and the COCH<sub>3</sub> bands (see orange and light blue 'spectra' in Fig. 11(a)) suggests the near complete decomposition of the PMMA film. Similar information could be obtained from the FTIR-RTM map processed as the CO/COCH<sub>3</sub> peak ratios and displayed as the image of chemical compositions (Fig. 11(b)). The variation in colors from pink to blue (from left to right) indicates the increase in the CO/COCH<sub>3</sub> (oxidation) and then the abrupt fall to white (equal to zero), which represents the complete degradation of the film. The FTIR-RTM map vividly represents the changes generated by the UV exposure; meanwhile, this graphical information also can be used as a supplement to interpret the results from the peel test addressed in Fig. 9, in which the peel force increases with the decrease of the contact angle.

#### 4. Conclusions

Using high-throughput peel tests of PMMA films from various metallic substrates, this study has demonstrated that the proposed combinatorial approach has the potential to characterize the interrelationship among the adhesion-



(a)



(b)

Fig. 11. Variations of carbonyl (CO) and ester (COCH<sub>3</sub>) band areas in FTIR spectra of PMMA films deposited on Al coated Si substrate as a function of UV exposure time (a), the corresponding IR image map (b).

controlling parameters rapidly, practically, and efficiently. The approach is expected to provide accurate results because of its large sampling space. In addition, using the proposed combinatorial peel test in conjunction with WLF equation, we have developed the annealing time–temperature superposition for determining the dependence of the critical contact angle to peel a film from a substrate (with a specific peel angle) on any arbitrary annealing time and temperature. Consequently, a master curve (a failure map) that relates the critical contact angle and the annealing time and temperature of the film/substrate system can be constructed. Furthermore, the proposed combinatorial peel test can be extended to construct master curves for other parameters relevant to peel adhesion (e.g. the dependence of peel force on any choice of temperatures and peeling rates).

## Acknowledgements

The authors would like to acknowledge Mrs K. Ashley

for the technical support during the sample preparation for FTIR experiment.

## References

- [1] Reddington E, Sapienza A, Gurau B, Viseanathan R, Sarangapani S, Smotkin E, Mallouk T. *Science* 1998;280:1735–8.
- [2] Wang J, Yoo Y, Gao C, Takeuchi I, Sun X-D, Chang H, Xiang X-D, Schultz PG. *Science* 1998;279:1712–3.
- [3] Sun XD, Xiang XD. *Appl Phys Lett* 1998;72:525–8.
- [4] Danielson E, Devenney M, Giaquinta DM, Golden JH, Haushalter RC, McFarland EW, Poojary DM, Reaves CM, Weinberg WH, Wu XD. *Science* 1998;279:837–9.
- [5] Jandeleit B, Schaefer DJ, Powers TS, Turner HW, Weinberg WH. *Angew Chem, Int Ed Engl* 1999;38:2494–7.
- [6] Klein J, Lehmann CW, Schmidt HW, Maier WF. *Angew Chem, Int Ed Engl* 1998;27:3369–74.
- [7] Brocchini S, James K, Tangpasuthadol V, Kohn J. *J Biomed Mater Res* 1998;42:66–72.
- [8] Dicknson TA, Walt DR, White J, Kauer JS. *Anal Chem* 1997;69:3413–9.

- [9] Newkome GR, Weis CD, Moorefiedl CN, Baker GR, Childs BJ, Epperson J. *Angew Chem, Int Ed Engl* 1998;37:307–11.
- [10] Gravert DJ, Datta A, Wentworth P, Janda KD. *J Am Chem Soc* 1998;120:9481–5.
- [11] Reynolds CH. *J Combinat Chem* 1999;1:297–304.
- [12] Takeuchi T, Fukuma D, Matsui J. *Anal Chem* 1999;71:285–93.
- [13] Schmitz C, Posch P, Thelakkat M, Schmidt HW. *Macromol Symp* 2000;154:209–21.
- [14] Gross M, Muller DC, Nothofer HG, Sherf U, Neher D, Brauchle C, Meerholz K. *Nature* 2000;405:661–4.
- [15] Meredith JC, Karim A, Amis EJ. *Macromolecules* 2000;33:5760–6.
- [16] Smith AP, Douglas J, Meredith JC, Karim A, Amis EJ. *Phys Rev Lett* 2001;87:15503–6.
- [17] Chiang MYM, Wu W, He JM, Amis EJ. *Thin Solid Films* 2003;437:197–203.
- [18] Chiang MYM, Song R, He JM, Karim A, Amis EJ. In: Kinloch AJ, editor. *Fracture of polymers, composites and adhesives*. Oxford: Elsevier; 2003.
- [19] Crosby AJ. *J Mater Sci* 2003;38:1–11.
- [20] Amis EJ. *Nat Mater* 2004;3:83–5.
- [21] Chiang MYM, Song R, Crosby AJ, Karim A, Chiang CK, Amis EJ. *Thin Solid Film* 2004 [in press].
- [22] Eidelman N, Simon CG. *J Res Natl Inst Stand Technol* 2004;109(2):219–31.
- [23] Lee I, Wool RP. *Macromolecules* 2000;33:2680–7.
- [24] Strawhecker KE, Kumar SK. *Macromolecules* 2001;34:4669–72.
- [25] Pfau A, Sander R, Kirsch S. *Langmuir* 2002;18:2880–8.
- [26] Williams ML, Landel RF, Ferry JD. *J Am Chem Soc* 1955;77:3701.
- [27] Chiang MYM, McKenna GB, Yuan J. *Polym Eng Sci* 1994;34:1815–22.
- [28] Fowkes FM. *Ind Eng Chem* 1964;56:40–8.
- [29] Horiuchi S, Fujita T, Hayakawa T, Nakao Y. *Adv Mater* 2003;15:1449–52.